EUROPEAN FUSION DEVELOPMENT AGREEMENT

EFDA–JET–PR(04)79

S.E. Sharapov, B. Alper, F. Andersson, Yu.F. Baranov, H.L. Berk, L. Bertalot, D. Borba, C. Boswell, B.N. Breizman, R. Buttery, C.D. Challis, M. de Baar, P. de Vries, L.-G. Eriksson, A. Fasoli, R. Galvao, V. Goloborod'ko, M.P. Gryaznevich, R.J. Hastie, N.C. Hawkes, P. Helander, V.G. Kiptily, G.J. Kramer, P.J. Lomas, J. Mailloux, M.J. Mantsinen, R. Martin, F. Nabais, M.F. Nave, R. Nazikian, J.-M. Noterdaeme, M.S. Pekker, S.D. Pinches, T. Pinfold, S.V. Popovichev, P. Sandquist, D. Stork, D. Testa, A. Tuccillo, I. Voitsekhovich, V. Yavorskij, N.P. Young, F. Zonca, the MAST Team and JET EFDA contributors

Experimental Studies of Instabilities and Confinement of Energetic Particles on JET and on MAST

Experimental Studies of Instabilities and Confinement of Energetic Particles on JET and on MAST

S.E. Sharapov[1], B. Alper[1], F. Andersson[2], Yu.F. Baranov[1], H.L. Berk[3], L. Bertalot[4], D. Borba[5], C. Boswell[6], B.N. Breizman[3], R. Buttery[1], C.D. Challis[1], M. de Baar[7], P. de Vries[1], L.-G. Eriksson[8], A. Fasoli[9], R. Galvao[10,5], V. Goloborod'ko[11,12], M.P. Gryaznevich[1], R.J. Hastie[1], N.C. Hawkes[1], P. Helander[1], V.G. Kiptily[1], G.J. Kramer[13], P.J. Lomas[1], J. Mailloux[1], M.J. Mantsinen[14], R. Martin[1], F. Nabais[5], M. F. Nave[5], R. Nazikian[13], J.-M. Noterdaeme[15,16], M.S. Pekker[3], S.D. Pinches[15], T. Pinfold[1], S.V. Popovichev[1], P. Sandquist[2], D. Stork[1], D. Testa[9], A. Tuccillo[4], I. Voitsekhovich[1], V. Yavorskij[11,12], N.P. Young[1,17], F. Zonca[4], the MAST Team and JET-EFDA Contributors*

[1]EURATOM/UKAEA Fusion Association, Culham Science Centre, Abingdon OX14 3DB, UK
[2]EURATOM/VR Fusion Association, Chalmers Univ. of Technology, Goteborg, Sweden
[3]Institute Fusion Studies, University of Texas at Austin, Austin, USA
[4]Association EURATOM/ENEA/CNR Fusione, Frascati, Italy
[5]EURATOM/IST Fusion Association, Centro de Fusao Nuclear, Lisboa, Portugal
[6] PSFC, Massachussets Institite of Technology, Cambridge, USA
[7]Association EURATOM-FOM Institute Plasmaphysics 'Rijnhuizen', Nieuwegein, The Netherlands
[8]Association EURATOM-CEA, CEA/DSM/DRFC, CEA Cadarache, F-13108 St Paul lez Durance, France
[9]CRPP/EPFL, Association EURATOM-Confederation Suisse, Lausanne, Switzerland
[10]Institute of Physics, University of Sao Paulo, Sao Paulo, Brazil
[11]Institute of Theoretical Physics, Association EURATOM-OEAW, University of Innsbruck, Austria
[12]Institute of Nuclear Research, Kiev, Ukraine
[13]Princeton Plasma Physics Laboratory, Princeton, USA
[14]Helsinki University of Technology, Association EURATOM-Tekes, Helsinki, Finland
[15] Max Planck Institute fur Plasmaphysik, EURATOM Association, Garching, Germany
[16]Gent University, Belgium
[17]University of Warwick, Coventry, UK
** See annex of J. Pamela et al, "Overview of JET Results ", (Proc.20 [th] IAEA Fusion Energy Conference, Vilamoura, Portugal (2004).*

Preprint of Paper to be submitted for publication in
Nuclear Fusion

ABSTRACT.

In preparation for next step burning plasma devices such as ITER, experimental studies of instabilities and confinement of energetic ions were performed on JET and on MAST, with innovative diagnostic techniques, in conventional and shear-reversed plasmas, exploring a wide range of effects for energetic ions. A compendium of recent results testing capabilities of the present-day facilities for burning plasma relevant study is presented in this paper. "Alpha tail" production using 3^{rd} harmonic ICRH of ^{4}He beam ions has been employed on JET for studying ^{4}He of the MeV energy range in a 'neutron-free' environment. The evolution of ICRH-accelerated ions of ^{4}He with $E \geq 1.7$MeV and D with $E \geq 500$keV was assessed from nuclear gamma-ray emission born by the fast ions colliding with Be and C impurities. A simultaneous measurement of spatial profiles of fast ^{4}He and fast D ions relevant to ITER were performed for the first time in positive and strongly reversed magnetic shear discharges. Time-resolved gamma-ray diagnostics for ICRH-accelerated ^{3}He and H minority ions allowed changes in the fast ion distribution function to be assessed in the presence of unstable toroidal Alfvén eigenmodes (TAEs) and sawteeth. A significant decrease of gamma-ray intensity from protons with $E \geq 5$MeV was detected during the "tornado" modes. This was interpreted as "tornado"-induced loss of fast ions with the drift orbit width, Δ_f, comparable to the minor radius of tokamak . Experiments performed in the opposite case, $\Delta_f/a \ll 1$, for ICRH-accelerated ^{3}He ions with $E \geq 500$keV, have shown excitation of numerous Alfvén eigenmodes without a significant degradation of the fast ion confinement. The stabilising effect of fast particles on "monster" sawteeth was experimentally found to fail in low-density plasmas with high power ICRF-heating. The transition from the "monster" to short-period "grassy" sawteeth was investigated with different ICRF phasing, that controls the pinch-effect and radial distribution of ICRF-accelerated ions. Instabilities excited by super-Alfvénic beam ions were investigated on the spherical tokamak MAST. Due to higher values of beta and a higher proportion of fast ions on MAST than on JET, a wider variety of modes and nonlinear regimes for the Alfvén instabilities were observed, including the explosive TAE-regimes leading to formation of hole-clump pairs on the fast ion distribution function. The MAST and START data showed that TAE and chirping modes decrease both in their mode amplitudes and in the number of unstable modes with increasing beta.

1. INTRODUCTION

Losses and redistribution of fast ions due to magnetic field topology and fast ion driven instabilities such as AlfvÈn Eigenmodes (AEs) and fishbones, as well as the fast particle effects on sawteeth represent major challenges for predicting with confidence plasma heating, fast ion dynamics and transport in next-step burning plasma devices such as ITER [1]. Although the complete and self-consistent investigation of a burning plasma is only possible in a burning plasma machine, the use of existing tokamak facilities can approach now some of the important problems, such as developing fast ion diagnostics and studying fast particle confinement. Two facilities, Joint European Torus (JET) and the Mega-Amper Spherical Tokamak (MAST), have been used for approaching the

problem of experimentally measuring fast particle profiles and confinement and for identifying characteristic instabilities driven with trapped and passing ions over wide range of plasma parameters. Aim of this paper is to present a survey of recent results demonstrating capabilities of the existing facilities in burning plasma relevant studies. More complete in-depth studies of every experiment described here require longer time and will be presented in future publications.

On JET, a trace tritium experiment was performed [2] in order to gain information on tritium transport and on fast ions [3, 4], and an "α-simulation" experiment similar to [5] was performed in helium plasma with significant population of ^{4}He ions accelerated to the MeV energy range with ICRF. The aim of the "α-simulation" experiment was to model the burning plasma, which will have several different groups of fast ions with comparable energy contents, but with essentially different distribution functions. In the case of ITER, these fast ions will be as follows: α-particles, deuterium Neutral Beam Injection (NBI) in the MeV range, and ions accelerated with Ion Cyclotron Resonance Frequency (ICRF) waves. In order to delineate the effects of α-particles and other fast ions under these conditions, simultaneous diagnosis of these fast ion populations with certain time and space resolutions is crucial and development of such diagnostics for burning plasmas is paramount. Diagnostics based on nuclear gamma-ray emission [6] from fast ions colliding with main plasma impurities, such as carbon and berillium, performed very well in JET trace tritium experiments [3], and were the focus of the "α-simulation" and some other experiments. A significant range of phenomena affecting fast ions of different types, i.e. ^{4}He, ^{3}He, D, and H, accelerated with ICRF-heating techniques, was explored. In the "a-simulation" experiment, the flexibility of the ICRF plant on JET was used for accelerating ITER-relevant fast ions of ^{4}He and D up to the MeV energy range [5].

Section 2 of this paper describes JET experiments on diagnosing multiple ICRF-heated fast ion populations via nuclear gamma-ray emission [6] in conventional and shear-reversed plasmas. The main problem of this experiment was to develop a scenario, in which the technique of ^{4}He beam acceleration with 3rd harmonic ICRF [5] could be combined with shear-reversed equilibrium in helium plasma. This problem has been successfully solved, and during this experiment simultaneous measurements of both ^{4}He and D fast ion profiles have been performed for the first time [7].

A search for plasma conditions leading to a significant loss of energetic ions in both the prompt orbit/classical collision regime and in the presence of TAEs was performed. Prompt orbit losses of fast ^{4}He in the form of "hot spots" on the first wall were observed in the "α-tail production" experiment in strong reversed shear equilibrium and these are discussed in Section 2. A strong decrease of gamma-ray emission coming from fast protons during the "tornado" mode activity (these modes are identified as TAEs within the $q = 1$ radius) has been detected in JET experiments with hydrogen minority ICRF-heating. This data are presented in Section 3.

Section 4 describes dedicated experiments aiming at time-resolved gamma-ray measurements of fast ^{3}He ions in the presence of unstable AEs in shear-reversed plasmas. The fast ion orbit width was quite small in this experiment, $\Delta_f/a << 1$, and in spite of numerous AEs excited with the fast

ions, no significant degradation of fast ions measured either by total intensity of the gamma-ray emission, or by detecting the hot spots at the first wall, was observed.

Section 5 describes JET experiments on further studies of sawteeth in low-density plasmas with high power ICRF-heating, when the fast ions fail to stabilise "monster" sawteeth [8]. A quite sharp threshold in plasma density was found to exist for the transition from a long-period monster sawtooth to a short-period and less regular "grassy" sawtooth. This transition to grassy sawteeth was found to correlate with stronger Fast Electron Bremsstrahlung (FEB) emission from supra-thermal electrons. Section 6 is devoted to instabilities excited by super-AlfvÈnic fast ions in NBI-heated plasmas on the spherical tokamak MAST. Due to higher values of β and a higher ratio of $\beta_{fast}/\beta_{thermal}$ on MAST, a wider variety of modes (including "chirping" modes [9, 10]) and nonlinear regimes for the instabilities were observed [11]. However, it was found experimentally that the number of unstable core-localised modes on MAST decreases with increasing $\beta_{thermal}$.

2. ALPHA-SIMULATION EXPERIMENTS IN SHEAR-REVERSED HELIUM PLASMAS

The development of burning / ignited plasma based on the reaction D + T $\rightarrow$ ^{4}He (3.5 MeV) + *n* (14MeV) requires a thorough investigation of fusion-born a-particles (^{4}He ions with birth energy 3.5MeV) in order to assess with confidence the a-particle behaviour in a DT power plant [1]. Previously, behaviour of a-particles has been studied successfully in full-scale DT experiments on the TFTR [12] and JET [13] tokamaks. It is however important to search for possible techniques of producing a significant population of ^{4}He ions in the MeV energy range in a non-activating plasma scenario without the complications of a full-scale DT campaign [5]. Such techniques could be of special importance for testing a-diagnostics and for obtaining information on confinement of ^{4}He ions in the relevant energy range in early non-activated phase of a reactor operation.

On JET, the ion-cyclotron resonance heating (ICRH) at the 3rd cyclotron harmonic of ^{4}He beam ions was successfully used for accelerating ^{4}He from 120 keV up to T_{He} ~1.1 ± 0.4MeV energy [5]. During such acceleration, a steady-state distribution function of fast ^{4}He ions with density $n_{He}^{fast}/n_e \approx 10^{-3}$ was obtained in 'neutron-free' (neutron rate $R_n \leq 10^{14}$sec^{-1}) helium H-mode plasmas with monotonic q(r)-profiles. The temperature and density of fast ^{4}He in these experiments were close to the obtained a-particle values in the record DT Pulse No: 42976 on JET, $T_\alpha \sim$ 1MeV, $n_\alpha/n_e \approx 4 \times 10^{-3}$, with neutron rate, $R_n \approx 5.7 \times 10^{18}$ sec^{-1} [13], but were obtained at four orders of magnitude lower neutron rates. In contrast to the real burning plasma, the ICRH discharges produce an anisotropic distribution function of ^{4}He with the fast ion profiles not determined by thermal ions as in burning plasma. Nevertheless, the 'α-production' technique [5] was found to be very useful for developing gamma-ray diagnostics [6, 7] of fast ^{4}He in the MeV range, and it significantly stimulated physics studies without the need in an expensive DT operation.

Here, we report on JET experiments combining the a-tail production technique [5] with strongly reversed magnetic shear and Current Holes (CH) [14, 15] scenarios targeting the Internal Transport

Barriers (ITBs). These scenarios were among the priority considerations for validating the physics of fast ^{4}He ions as the confinement of α-particles may be vulnerable in such regimes [16, 17] and direct experimental observations of confined fast ions are highly desirable.

Figure 1 shows the typical waveforms of high-power ICRH applied at 51MHz in order to accelerate the low-power "seed" ^{4}He beam with energy 110keV, that efficiently couples to the RF-wave because of the beam particle finite Larmor radius. LHCD was applied during the inductive current ramp-up in order to obtain strong-reversed shear equilibrium, while the magnetic field ramp-up is used for increasing the coupling of LHCD. In the absence of the MSE measurements in these helium plasma and helium NBI discharges, MHD spectroscopy based on Alfvén Cascades (ACs) [18-20] shown in Figure 2 and on strong-reversed-shear sawteeth [21] was the main indicator of the shear-reversal equilibrium. Spatial profiles of ^{4}He ions with energy >1.7MeV were measured in discharges with monotonic (Fig.3a) and non-monotonic (Fig.3b) q(r)-profiles. These measurements were performed with a 19-channel 2D camera detecting nuclear gamma-rays born in the reaction ^{9}Be (^{4}He, ng)^{12}C between $\approx$ 1.9MeV (peak cross-section) ions of ^{4}He and Be impurity [6] with an integration time 1 sec. The measured profiles agree well with the topology of fast ion orbits in positive (banana-shape) and strongly reversed shear (vertical drift through the plasma centre) discharges in Figs. 4a and 4b correspondingly. The somewhat hollow profile of ^{4}He fast ions in Fig. 4a is also confirmed by observations of unstable TAEs with negative toroidal mode numbers, $n = -1, -2$ driven by a reverse gradient of the fast ion pressure. The hollowness of the fast ^{4}He profile is attributed to the use of almost tangential "seed" ^{4}He NBI, whose perpendicular velocity component is small at the magnetic axis. In this geometry, only beam at a certain distance from the magnetic axis can be accelerated through the finite Larmor radius effect crucial for the 3rd harmonic ICRF-heating.

In addition to the beam ^{4}He ions, some parasitic absorption of ICRH power was caused by the 3rd ICRH harmonic of thermal deuterium minority ions with density $n_D/n_e \approx 10\%$. The combined effect of ^{4}He beam and D minority acceleration with ICRH has allowed a demonstration for the first time simultaneous measurements of spatial profiles of fast ^{4}He with E $\geq$ 1.7MeV (Fig.3a) and fast D ions with E $\geq$ 500 keV (Fig. 3c) with the gamma-ray tomography. These types of fast ions are highly relevant for the ITER scenarios, in which 1MeV deuterium negative NBI will co-exist with fusion-born a-particles. These proof-of-principle simultaneous measurements of fast D and ^{4}He ions performed in a neutron-free environment are strongly encouraging for further development of radiation-resistant detectors and neutron filters allowing similar gamma-ray measurements during DT operation [22].

The 3rd ICRH-harmonic acceleration of a ^{4}He beam was found to depend strongly on the beam energy. Figure 5 shows energy spectra of gamma-ray emission measured in identical helium JET discharges, but with a single NBI source of ^{4}He changed from 110keV to 70keV. It is seen that such substitution does not affect the spectral line of gamma-rays at 3.1MeV, which is caused by fast minority deuterium colliding with carbon. At the same time, the spectral line of 4.44MeV gamma-ray emission caused by ^{4}He with E $\geq$ 1.7MeV colliding with Be impurity is only seen in the discharge

with 110keV, while the discharge with 70keV NBI has much weaker intensity of this line. This observation is in good agreement with the previously published results on comparison of ICRH acceleration of 120keV and 70keV ^{4}He beams [5].

Although JET was not equipped with lost fast ion diagnostics, a significant flux of escaping fast ^{4}He ions could be deduced from experimentally observed severe hot spots seen as regions of bright visible light coming mostly from the equatorial zone of poloidal limiters, about 20cm in size. A scan of the plasma currents through the range I_p^{max}= 1.5÷2MA (for B_0 = 2.2T) was performed to determine the current needed to moderate fast ion losses. A tolerable level of the losses (such that the hot spots were only present at heat-protected plates of the wall) was found only at the highest current scanned, 2MA. This relatively high current needed for moderating the orbit losses could be explained by a low-current region/ current hole of radius up to $r_{CH} \approx 0.2$ a existing in these reversed-shear discharges, and thus re-normalising critical value of the total current as [17]

$$I_{crit}[MA] \cong \frac{0.55 \cdot I_{crit}^{mono}[MA]}{1-\sqrt{r_{CH}/a}} \cong \frac{1.4}{Z_i}\sqrt{\frac{\mu_i E[MeV]}{(R_0/a)}} \times \frac{1}{1-\sqrt{r_{CH}/a}}. \qquad (1)$$

With the 2D gamma-ray tomography, it was also possible to observe a time-averaged (integration time 1 sec) effect of the q=1 sawtooth oscillations on the radial profile of ^{4}He ions. It was found that a transition from non-sawtoothing to sawtoothing plasma broadens the radial profile of the fast ions by ~5-10cm. In the case of the SRS sawteeth, a tendency to a better confinement of fast ions was observed after the transition from the SRS-sawtoothing plasma to non-sawtoothing plasma, but a higher number of gamma-ray counts is needed in order to justify such effect statistically.

3. TAE-INDUCED LOSSES OF ICRH-ACCELERATED PROTONS WITH E > 5MEV ON JET

A search for TAE-induced losses of ICRF-accelerated ions has been performed with the use of gamma-ray diagnostics for JET discharges with hydrogen minority ICRF-heating, which is the most common and well-established scenario on JET. In the past, significant losses of ICRH-accelerated fast protons and degradation of total plasma energy content caused by the so-called "tornado" modes at the TAE-frequency range were first detected on JT-60U and reported in [23]. A neutron counter was used on JT-60U in order to measure the time evolution of the fast protons with energy E ≥ 3MeV from the nuclear reaction ^{11}B(p,n)^{11}C. Conclusions on significant loss of fast ions were then drawn based on the observed loss of monster sawtooth stabilisation by the fast ions during TAE and tornado mode activity on DIII-D [24, 25] and on TFTR [26]. More recently, tornado modes were observed for the first time on JET. These were identified as core-localised TAEs [27], and the condition for their existence within the $q = 1$ radius was identified to be: $r(q=1)/R_0 < S$, where r(q=1) is the minor radius, at which magnetic surface q=1 is localised, S is the magnetic shear at q=1, and R_0 is the major radius of the magnetic axis [28].

Fast particle losses / redistribution similar to these observed on JT-60U and deduced on TFTR and DIII-D were found on JET as a significant (by a factor of two) decrease of gamma-ray emission coming from the nuclear reaction $^{12}C(p, p'\gamma)^{12}C$ during the combined activity of tornado (inside the $q = 1$ radius) and TAE (outside the $q = 1$ radius). Here, the gamma-ray emission is induced by protons accelerated with ICRF minority heating up to the energy range >5MeV. Figure 6 shows a sudden and significant decrease of the intensity of the gamma-ray emission observed with gamma-spectrometer in JET discharge (Pulse No: 60195) with B_0= 2.7T, $I_P \approx$ 2MA, at t ≈ 10.5sec and t ≈ 12sec. The decrease of the gamma-ray intensity starts during a sawtooth-free period at steady-state ICRF heating, about 0.5 ÷ 1sec before monster sawtooth crashes seen in Figure 7. It correlates in time with tornado modes and TAEs detected with external magnetic pick-up coils as Figs. 8 and 9 show. Two different sets of modes in Figs. 8, 9 are the TAEs with nearly constant frequencies and the tornado modes with frequencies sweeping down as q(0) decreases.

Analysis of the Alfvén Eigenmode spectrum in the reconstructed equilibrium was performed with the ideal MHD MISHKA code [29], and the computed eigenfunctions of the AEs with toroidal mode numbers matching observed modes at t = 13sec are shown in Figure 10. One can see that the combination of the TAEs inside the q = 1 radius (tornado) and outside the q = 1 radius form a TAE-"corridor" that spreads from the central to a half-radius of the plasma. Prompt losses of the trapped protons with $E > 5$ MeV with orbit width up to $\Delta f/a \leq 0.5$ (Figure 11) significantly enhanced by the TAEs are considered as a primary channel of the proton losses in this case, and the relevant modelling of such losses will be published elsewhere.

4. TIME-RESOLVED MEASUREMENTS OF ICRF-ACCELERATED ^{3}HE IONS WITH E > 500 KEV ON JET

In order to study coupling between fast ions and Alfvén Eigenmodes in the regime of small drift orbits of fast ions, $\Delta_f/a \approx 0.1 << 1$, relevant for ITER-type machines, JET developed a scenario for Alfvén Eigenmodes excited with ICRF-accelerated ^{3}He minority in ^{4}He plasma. Fast ^{3}He ions with energy as low as 500keV can interact with C and Be impurities and generate gamma-rays through nuclear reactions much more numerous than ^{4}He [6]. Due to the high intensity of this gamma-ray emission from ^{3}He, time-resolved measurements of fast ^{3}He become possible. The choice of a helium plasma instead of deuterium was determined by two main reasons. First, for similar ion temperatures, ^{4}He thermal ions have lower speed than deuterium thermal ions, so that the ion Landau damping of AEs due to the $V_{||i} = V_A/3$ resonance is exponentially smaller for AEs in ^{4}He plasma. Second, the low level of neutrons makes the gamma-ray measurements nearly noise-free, so a better quality gamma-ray images of the fast ^{3}He ions with time resolution up to 10 msec, could be obtained.

Figure 12 shows simultaneous measurements of the AE activity in the frequency range up to 450kHz with Mirnov coil, together with the intensity of gamma-ray emission measured by the vertical gamma-ray camera in JET helium Pulse No: 63099. In this discharge, the magnetic field

and maximum plasma current were B = 3.3T, I = 2.3MA respectively, electron temperature and density were $T_e(0) \approx 6.5$keV, $n_e(0) \approx 2.5\times10^{19}$ m^{-3}, and the plasma composition was ^{4}He:D = 91% : 9%. LHCD power of 1.7MW was applied during the current ramp-up phase in order to obtain a reversed shear magnetic configuration, and ICRF power of 5MW was applied for the on-axis heating of ^{3}He minority ions. Notches in the ICRF power from 5MW down to 1MW were performed in this discharge in order to observe both the decay and increase of the ^{3}He fast ion population with $E >$ 500keV on the gamma-ray diagnostics. It is seen in Figure 12 that numerous Alfvén Eigenmodes of different types were excited in this discharge: Alfvén Cascades, TAEs, and EAEs. The notches in ICRF power affect significantly both the gamma-ray emission from ^{3}He ions, and the AEs, but different AEs are affected somewhat differently. Figure 13 shows that a sharp decrease in intensity of gamma-ray emission from ^{3}He with $E >$ 500keV is well correlated with the disappearance of the TAE modes. However, the Alfvén Cascades with frequencies approaching the TAE persist during the time of the notch in ICRF power, when no ^{3}He ions are detected with the gamma-ray camera. This indicates that the AC instability is caused by ^{3}He ions with energies lower than 500 keV, in some correspondence with the observation of ACs on JET and on DIII-D driven with sub-Alfvénic NBI [30]. In spite of the high amplitude AE activity in the whole frequency range covered by the MHD diagnostics, the time-resolved measurements of ^{3}He with $E >$ 500 keV detected no notable degradation of gamma-ray emission due to any of the AEs observed in these discharges with the orbit widths $\Delta_f / a << 1$.

5. GRASSY SAWTEETH IN LOW-DENSITY JET DISCHARGES

Fast particles play a major role in the q = 1 sawtooth stabilisation, and the effect of alpha-particles on sawteeth in burning plasma is one of the most important problems of burning plasma [31]. It was discovered some time ago on JET that in plasmas of low density, $n_e \le n_e^{crit} \approx 2\times10^{19}$ m^{-3}, with high-power ICRF-heating the ICRH-accelerated ions fail to stabilise sawteeth even though the fast ion energy content could be comparable to that of thermal plasma [8]. With plasma density decreasing, discharges abruptly change from the usual monster sawtooth regime to a regime with very short period and more chaotic “grassy” sawteeth as soon as the threshold in density is passed. These grassy sawteeth are accompanied by higher-frequency activity, n = 1 fishbone-like modes [31, 32] and AEs. Possible explanations for the loss of fast ion stabilising effect were searched for and the orbit width of the fast ions exceeding the q = 1 radius [33] and possible generation of supra-thermal electrons during sawtooth crashes similar to [34] were identified as the main density-dependent effects. In order to investigate these effects, dedicated experiments were performed in JET low-density plasmas with high power, P > 4 MW, ICRF-heating of hydrogen minority ions. The effect of fast ion profiles on sawteeth was studied with on- and off-axis ICRH and with ICRH launched co- and counter-current. Figures 14 (a-c) show typical time traces of electron temperature in JET discharges with ICRF hydrogen minority heating with (a) dipole; (b) $+90^o$ phasing of the ICRH antenna, and (c) -90^o phasing. The wave with $+90^o$ phasing corresponds to the co-current direction

and it generates a more peaked radial profile of fast ions with higher temperature [35, 36]), while the wave launched in the counter-current direction (-90^0) produces a flattish radial profile of the fast ions with lower temperature. In all three cases sawteeth with periods shorter than monster sawtooth period were obtained, in spite of the different radial profiles and temperatures of fast ions. However, these three cases show a distinctly different behaviour of the cold kink perturbation (seen as oscillatory structure), and cannot be counted as a single grassy sawtooth phenomenon and should be studied separately.

Although the grassy sawteeth were found to be very sensitive to the details of fast ion profiles, it was difficult to associate the very sharp density threshold triggering the transition to grassy sawteeth in terms of values associated with fast ions such as the slowing down time of these ions. The only phenomenon with which the sharp transition to grassy sawteeth was found to correlate, was the intensity of Fast Electron Bremsstrahlung (FEB) emission from central region of plasma as Figure 15 shows. Measurements of supra-thermal electron emission in the energy range from 150keV to 450keV were made with fast electron bremsstrahlung camera with the lines-of-sight through the central region of the plasma at 90^o angle with respect to the magnetic axis. These measurements show a significant increase of the suprathermal electron emission just before the transition to grassy sawteeth. Bursts of supra-thermal ECE emission is also seen during the sawtooth crashes. Estimates show that in these low-density high-temperature discharges the electric field was close to the critical field for the runaway electrons, $E \approx E_{crit}$, so the sawtooth crashes could affect the runaways by generating electric field comparable to the near-threshold value $E_{crit} - E$. The observations of the enhanced FEB emission indicate that supra-thermal electrons may carry a significant current in vicinity of the $q = 1$ magnetic flux surface and play a role in sawtooth dynamics, which was never investigated in the past and may constitute a new problem in this field.

6. ALFVÈN EIGENMODES IN HIGH-B SPHERICAL TOKAMAKS

Very important data on fast ion-driven modes has been obtained on the spherical tokamak MAST. The low toroidal magnetic field, $B < 0.5$ T, of the STs makes MAST a perfect test bed for studying energetic particle driven modes due to the super-Alfvénic nature of NBI at energy as low as 30keV [11]. Many Alfvén instabilities excited by NBI-produced energetic ions have been observed on MAST: fixed-frequency modes in the TAE and EAE frequency ranges, frequency-sweeping "chirping" modes similar to these observed on DIII-D [9] and on START [10], fishbones, and modes with frequencies above the AE frequency range. The key ratio that determines the perturbative versus non-perturbative type of the mode $\beta_{fast}/\beta_{thermal}$, in Spherical Tokamak (ST) can be higher than that usually obtained in other tokamaks. The record value of volume-averaged β @ 40%, achieved in START NBI-heated plasmas and the concept of high-β burning plasma STs being considered [37] makes it necessary to consider the role of thermal and fast ions in the electromagnetic instabilities. The problem of a dominant fast ion driven instability at high-β was assessed on MAST experimentally and a similar analysis of earlier data from START was performed. The data shows that the two

major pressure-gradient driven fast ion instabilities, core-localised TAEs and chirping modes decrease both in mode amplitudes and in the number of unstable modes with increasing β [11]. On START, the chirping mode amplitude decreases as β increases as Figure 16 shows. Chirping modes disappear as β increases and they have not been observed in high-β discharges. The initial increase of the mode amplitude with β-increase is caused by the increase in the fast ion pressure. Figure 17 shows that a similar tendency to the chirping mode disappearance at higher β is observed on MAST.

Theoretical consideration of the pressure effect on TAE-modes was investigated in [11]. It was shown that the experimentally observed β-threshold for the observations of core-localised TAE can be explained by the pressure effect on the existence of TAEs. The suppression of the core-localised TAEs by high plasma pressure happens close to the threshold values of the plasma pressure parameter [27].

$$\alpha = \alpha_{crit}^{\pm} = \varepsilon + 2\Delta' \mathbf{m} S^2,$$

where $e = r / R_0$; Δ' is the Shafranov shift derivative Δ'; S is the magnetic shear value, and $a = -R_0 q^2 d\beta/dr$ is the normalised pressure gradient, and the signs + and – correspond to the upper core-localised TAE and the lower core-localised TAE [27] correspondingly.

The importance of fast-ion driven instabilities in burning plasma spherical tokamaks, which would necessarily operate in high-beta regimes, has to be further investigated both experimentally and theoretically although it is expected that many of the numerous energetic-particle-driven instabilities observed at low-beta in present-day machines will be absent in the higher-beta burning plasma devices.

SUMMARY

In order to assess the capabilities of investigating some important problems relevant for future burning plasma devices on present-day devices, a number of experiments were performed on JET and MAST. The problem of exploiting the existing facilities for studying fast particles required both development of new scenarios and investigation of previously unexplored data relevant for the fast particle physics. A survey of the experiments devoted to the fast particles on present-day tokamaks JET and MAST presented here demonstrates several important avenues along which the preparation to the real burning plasma experiment may proceed.

Direct measurements of profiles and energy spectra of ^{4}He, ^{3}He, D and H ions accelerated with ICRF were performed on JET with gamma-ray diagnostics [6]. Alpha tail production using the 3rd harmonic ICRF-heating of ^{4}He beam ions in ^{4}He plasmas has been employed for studies of the gamma-ray diagnostics of ^{4}He ions in the MeV energy range in a 'neutron-free' environment, in plasmas with monotonic and non-monotonic q(r)-profiles. Simultaneous measurements of spatial profiles of fast ^{4}He and fast D ions relevant to ITER were performed for the first time and they were found to be in agreement with the theory of fast ion orbits in positive and strongly reversed magnetic shear discharges.

A strong decrease of gamma-ray emission caused by ICRF-accelerated protons with energy exceeding 5MeV was detected during the tornado mode activity on JET. Although similar data have been earlier reported fron JT-60U, DIII-D, and TFTR machines, this is the first observation of such phenomenon on JET. The gamma-ray decrease is interpreted as tornado-enhancement of prompt orbit loss of fast ions with orbit width comparable to the minor radius of the machine.

Time-resolved measurements of fast ^{3}He ion profiles were performed in the opposite limit of fast ion orbit width much smaller than the minor radius with a time resolution up to 10 msec. This data allows assessment of (a) the stability of the excited modes based on the *measured* profiles and (b) the coupling between Alfvén modes with different frequencies and the fast ions.

The effects of ICRH-accelerated ions and supra-thermal electrons on sawteeth of very short periods (grassy sawteeth) and their transition to monster sawteeth at increasing plasma density were experimentally assessed. The effect of fast ion profiles on sawteeth was studied with ICRF waves launched co- and counter-current.

Data on fast ion-driven modes in the tight aspect ratio MAST and START experiments with super-Alfvénic NBI show that core-localised TAEs and chirping modes decrease both in the mode amplitudes and in the number of unstable modes with increasing beta. A very interesting and important problem of the hierarchy between different types of fast-ion driven instabilities in burning plasma STs, which would necessarily operate in high-beta regimes, arises and should be investigated further both experimentally and theoretically.

Together with the full-scale DT experiments with real alpha-particles, which demonstrated plasma heating by the alpha-particles [38], investigated ion-cyclotron [39] and Alfvén [40] instabilities driven by alpha-particles, and established the knock-on effects caused by alpha-particles [41], the experiments described here provide an important milestone in a further planning of developing diagnostics and directions for experimental and theoretical studies aiming at the burning plasma.

ACKNOWLEDGMENTS

It is pleasure to thank our colleagues at JET and MAST who operated the tokamaks, the heating systems and the diagnostics during these experiments. Valuable discussions with W.W.Heidbrink and K.-L.Wong visiting JET at the time of the experiments are highly appreciated. The work was performed under the European Fusion Development Agreement and was partly funded by Euratom and the UK Engineering and Physical Sciences Research Council.

REFERENCES

[1]. ITER Physics Basis, Nuclear Fusion 39 (1999) 2137

[2]. Stork D. *et al.*, Fusion Energy 2004 (Proc. 20th Int. Conf. Vilamoura, 2004) (Vienna: IAEA), paper OV/4-1 (http://www-naweb.iaea.org/napc/physics/fec/fec2004/datasets/index.html)

[3]. Kiptily V.G. *et al.*, Phys. Rev. Lett. **93** (2004) 115001

[4]. Hawkes N.C. *et al., Tritium fast ion distribution in JET current hole plasmas,* submitted to Plasma Physics Control. Fusion (2005)
[5]. Mantsinen M.J. *et al*., Phys. Rev. Lett. **88** (2002) 105002
[6]. Kiptily V. G. *et al*., Nuclear Fusion **42** (2002) 999
[7]. Kiptily V. G. *et al.*, Nuclear Fusion **45** (2005) L21
[8]. Mantsinen M.J. *et al*., Plasma Phys. Control. Fusion **42** (2000) 1291
[9]. Heidbrink W.W. Plasma Phys. Control. Fusion **37** (1995) 937
[10]. Gryaznevich M.P. and Sharapov S.E. Nuclear Fusion **40** (2000) 907
[11]. Gryaznevich M.P. and Sharapov S.E. Plasma Phys. Control. Fusion **46** (2004) S15
[12]. Hawryluk R.J. *et al.*, Phys. Rev. Lett. **72** (1994) 3530
[13]. Keilhacker M. Phil. Trans. R. Soc. London A **357** (1999) 415
[14]. Hawkes N. *et al*., Phys. Rev. Lett. **87** (2001) 115001
[15]. Fujita T *et al*., Phys. Rev. Lett. **87** (2001) 245001
[16]. Yavorskij V. *et al*., Nuclear Fusion **43** (2003) 1077
[17]. Yavorskij V *et al*., Nuclear Fusion **44** (2004) L5
[18]. Sharapov S.E. *et al*., Phys. Letters **A289** (2001) 127
[19]. Berk H.L. *et al*., Phys. Rev. Lett. **87** (2001) 185002
[20]. Sharapov S.E. *et al*., Phys. Rev. Lett. **93** (2004) 165001
[21]. Challis C.D. *et al*., Plasma Phys. Control Fusion **43** (2001) 861
[22]. Kiptily V.G. *et al.*, Plasma Devices and Operations **7** (1999) 255
[23]. Saigusa M. *et al*., Plasma Phys. Control. Fusion **40** (1998) 1647
[24]. Heidbrink W.W. *et al*., Nuclear Fusion **39** (1999) 1369
[25]. Bernabei S. *et al*., Nuclear Fusion **41** (2001) 513
[26]. Bernabei S. *et al*., Phys. Rev. Lett. **84** (2000) 1212
[27]. Berk H.L. *et al*., Phys. Plasmas **2** (1995) 3401
[28]. Kramer G.J. *et al*., Phys. Rev. Lett. **92** (2004) 015001
[29]. Mikhailovskii A.B. *et al*., Plasma Phys. Reports **23** (1997) 844
[30]. Nazikian R. *et al*., Fusion Energy 2004 (Proc. 20th Int. Conf. Vilamoura, 2004) (Vienna: IAEA), paper EX/5-1 (http://www-naweb.iaea.org/napc/physics/fec/fec2004/datasets/index.html) [31] Porcelli F. *et al*., Phys. Plasmas **3** (1994) 470
[32]. Gorelenkov N.N. *et al*., Fusion Energy 2004 (Proc. 20th Int. Conf. Vilamoura, 2004) (Vienna: IAEA), paper TH/5-2Rb (http://www-naweb.iaea.org/napc/physics/fec/fec2004/datasets/index.html)
[33]. Nabais F. *et al*, Fusion Energy 2004 (Proc. 20th Int. Conf. Vilamoura, 2004) (Vienna: IAEA), paper TH/5-3 (http://www-naweb.iaea.org/napc/physics/fec/fec2004/datasets/index.html)
[34]. Savrukhin P.V. Phys. Rev. Lett. **86** (2001) 3036
[35]. Eriksson L.-G. *et al*., Phys. Rev. Lett. **81** (1998) 1231
[36]. Mantsinen M.J. *et al*., Phys. Rev. **89** (2002) 115004

[37]. Wilson H. *et al.*, Fusion Energy 2004 (Proc. 20th Int. Conf. Vilamoura, 2004) (Vienna: IAEA), paper FT/3-1Ra (http://www-naweb.iaea.org/napc/physics/fec/fec2004/datasets/index.html)
[38]. Thomas P.R. *et al.*, Phys. Rev. Lett. **80** (1998) 5548
[39]. McClements K.G. *et al.*, Phys. Rev. Lett. **82** (1999) 2099
[40]. Sharapov S.E. *et al.*, Nucl. Fusion **39** (1999) 373
[41]. Zaitsev F.S. *et al.*, Nucl. Fusion **42** (2002) 1340

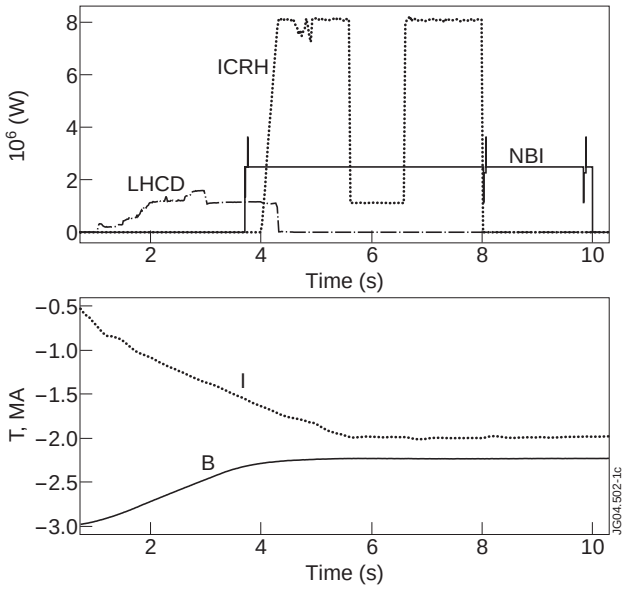

Figure 1: Top: power waveforms of LHCD, ICRH, and ^{4}He NBI in JET Pulse No: 63038. Bottom: inductive current and toroidal magnetic field.

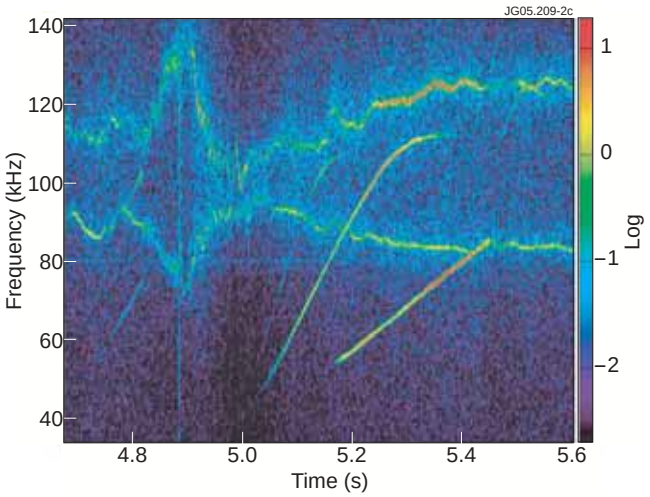

Figure 2: Magnetic spectrogram showing Alfvén Cascades and SRS sawtooth (vertical line at t= 4.8sec) in JET Pulse No: 63038.

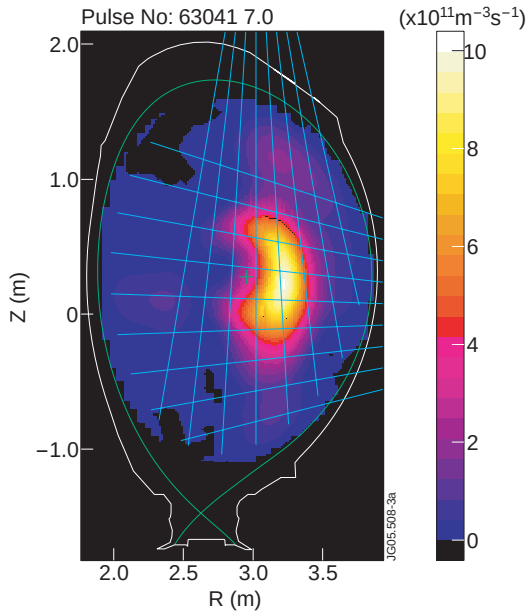

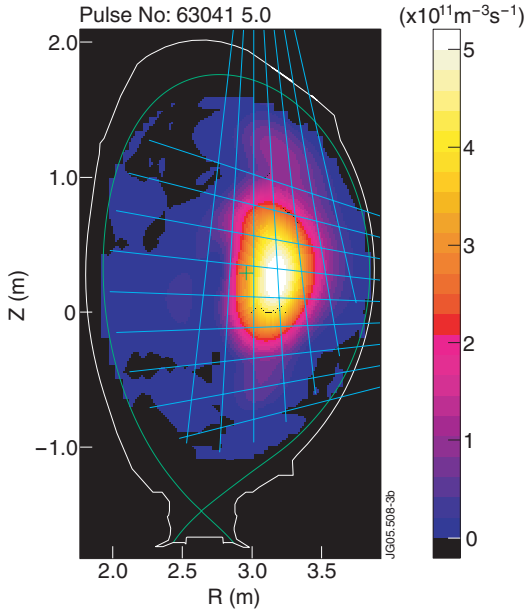

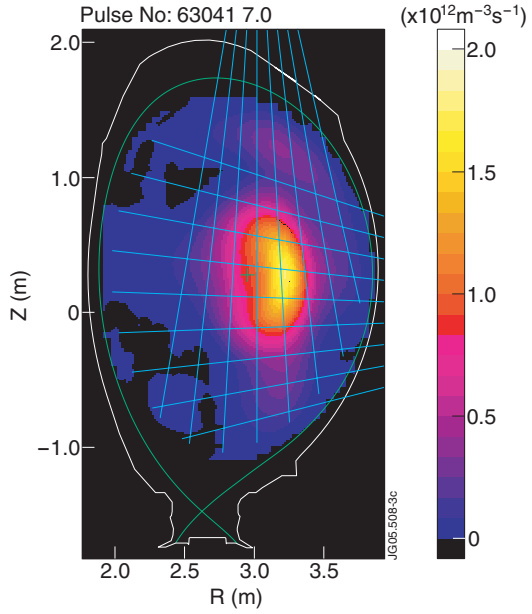

Figure 3(a): Profile of gamma-ray emission from ^{4}He ions in case of monotonic q(r)-profile. Figure 3(b): Profile of gamma-ray emission from ^{4}He ions in strongly reversed shear case. Figure 3(c): Profile of gamma-ray emission from D ions in case of monotonic q(r)-profile.

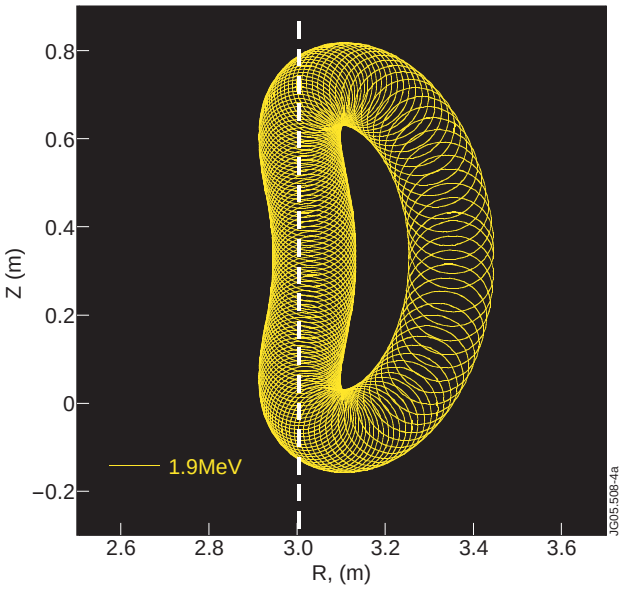

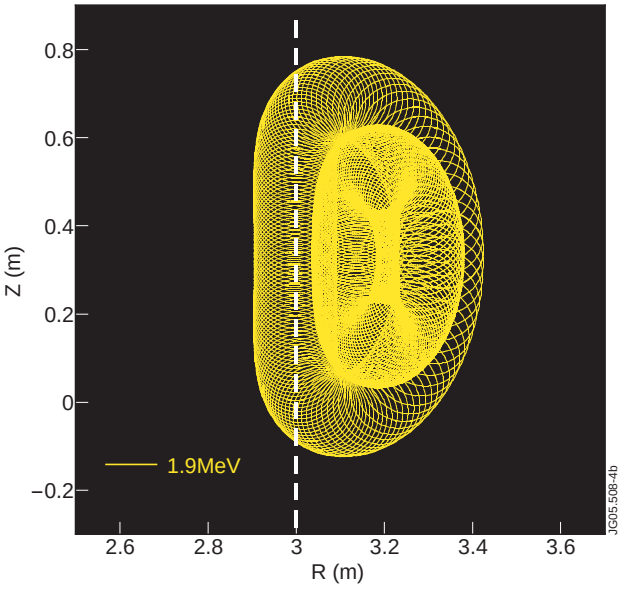

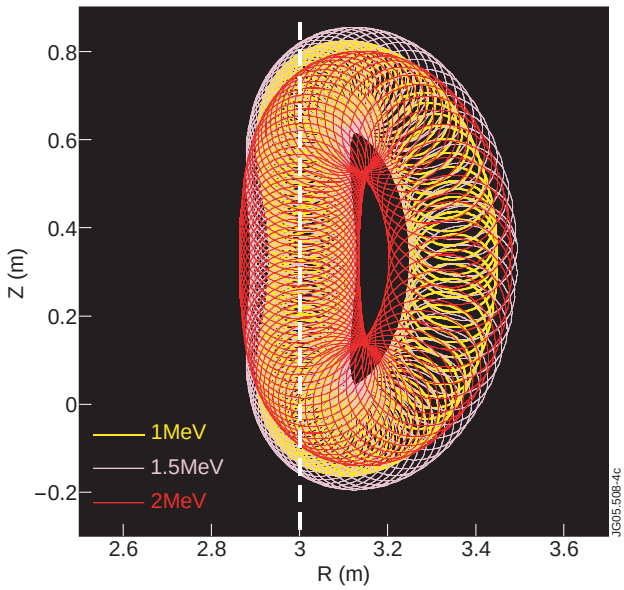

Figure 4(a): ICRH-accelerated ^{4}He ion orbit for Fig.3(a)
Figure 4(b): ICRH-accelerated ^{4}He ion orbit for Fig.3(a).
Figure 4(c): ICRH-accelerated D ion orbit for Fig.3(c).

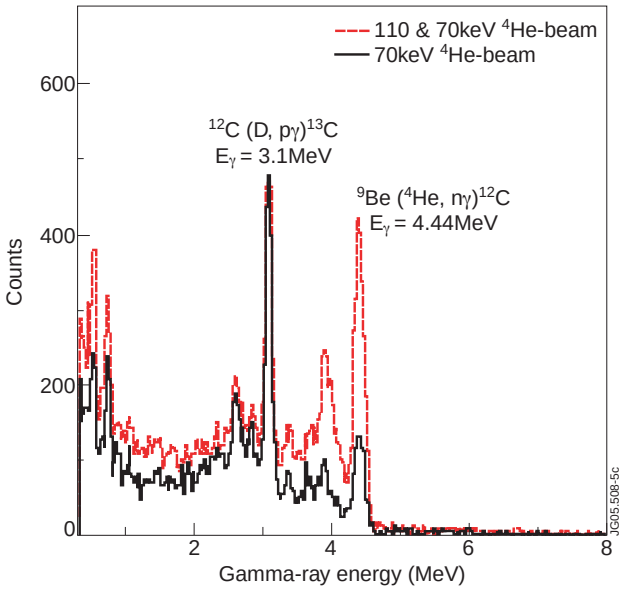

Figure 5: Gamma-ray spectra recorded in JET discharges with identical plasma parameters, but with different energy "seed" ^{4}He NBI (110keV and 70keV). Main spectral lines correspond to gamma-ray emission from ^{4}He (E>1.7MeV) + Be and from D (E>500keV) + C reactions.

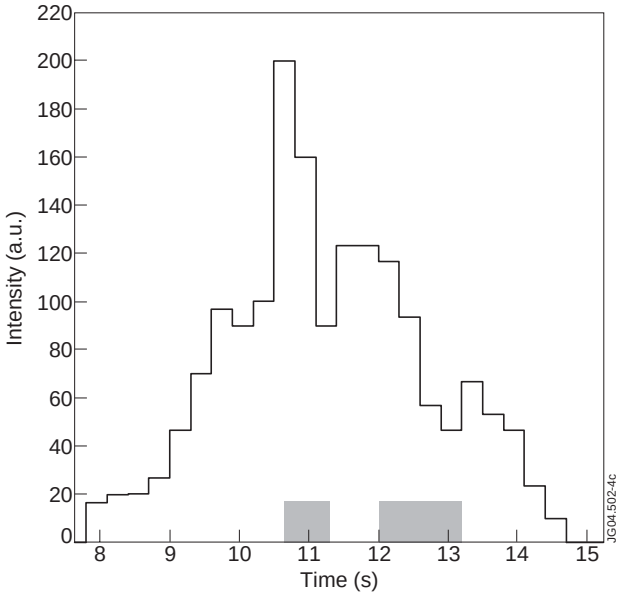

Figure 6: Intensity of γ-rays born in nuclear reactions between fast H and C as measured with vertical γ-ray spectrometer in JET plasma. Shaded areas mark gamma-degradation periods.

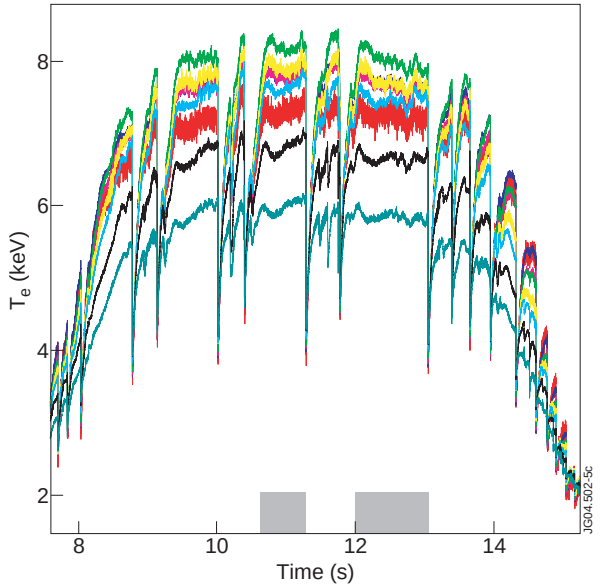

*Figure 7: Electron temperaturse measured by multi-channel ECE at different radii. Monster sawteeth at t=11.4 and t=13s occur **after** degradation of gamma- intensity marked as shaded time intervals.*

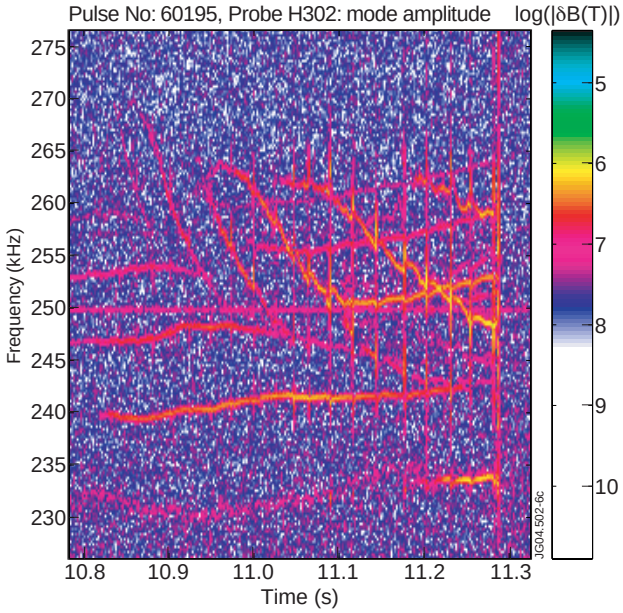

Figure 8: Magnetic spectrogram showing amplitude of TAEs & tornadoes as function of time and frequency (first shaded time interval in Fig.7).

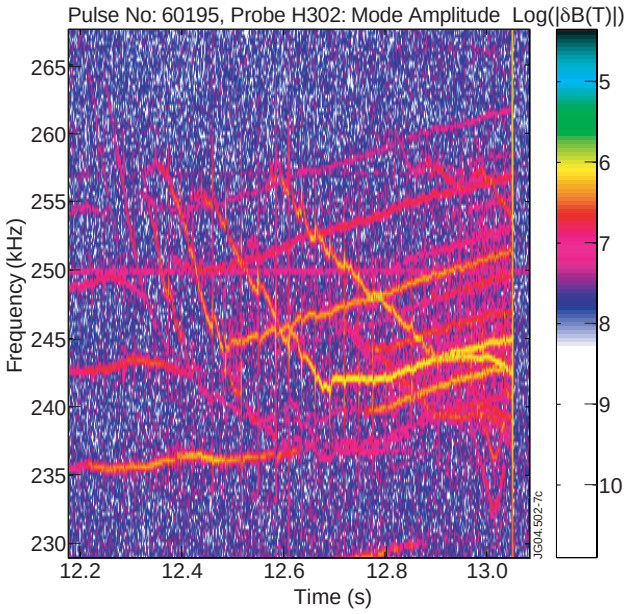

Figure 9: Magnetic spectrogram showing amplitude of TAEs & tornadoes as function of time and frequency (second shaded time interval in Fig.7).

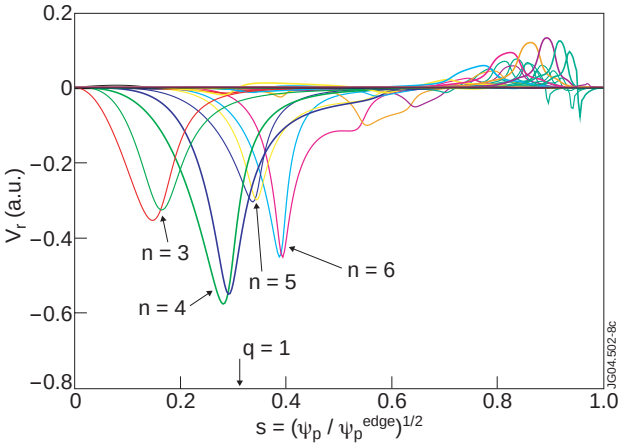

Figure 10: Core-localised TAEs with n=3, 4 and eigenfunctions within q=1 radius (tornado), and n=5,6 TAEs outside q=1 computed for JET equilibrium in Pulse No: 60195 at t=13sec.

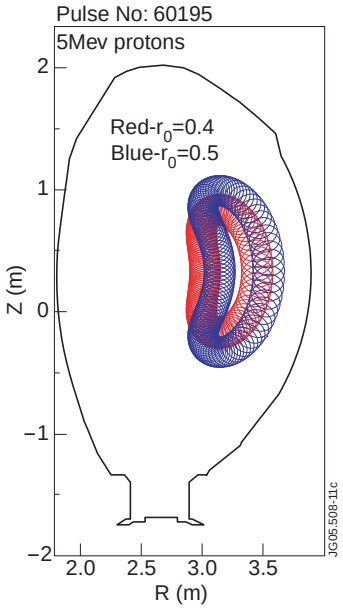

Figure 11: Orbits of 5MeV protons accelerated with on-axis ICRH in JET Pulse No: 60195.

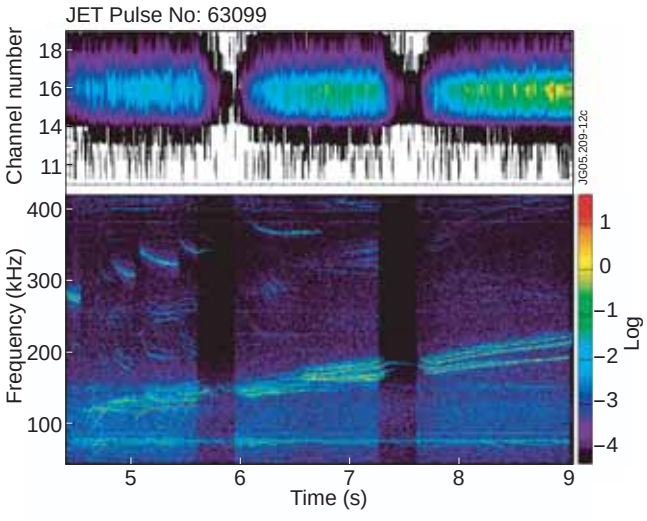

Figure 12: Top: intensity of γ-rays born in nuclear reactions between fast ^{3}He and Be as measured with vertical γ-ray camera (channel 11 is at the inner side of the torus and channel 19 at the outer side). Bottom: Magnetic spectrogram showing Alfvén Cascades, TAEs and EAEs excited by fast ^{3}He ions at the time of measurements of the ^{3}He profile (Pulse No: 63099).

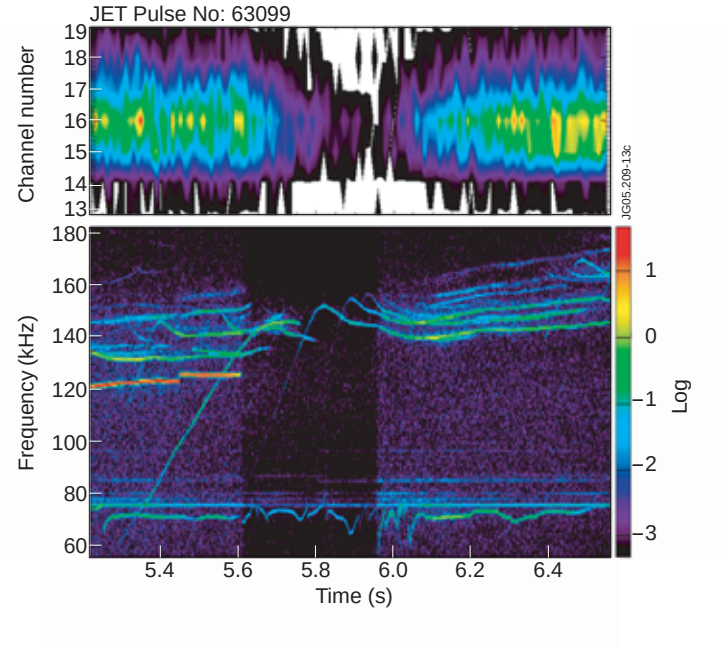

Figure 13: Zoom of Figure 12: Top: intensity of γ-rays born in nuclear reactions between fast ^{3}He and Be. Bottom: Magnetic spectrogram showing Alfvén Cascades and TAEs excited by fast ^{3}He ions.

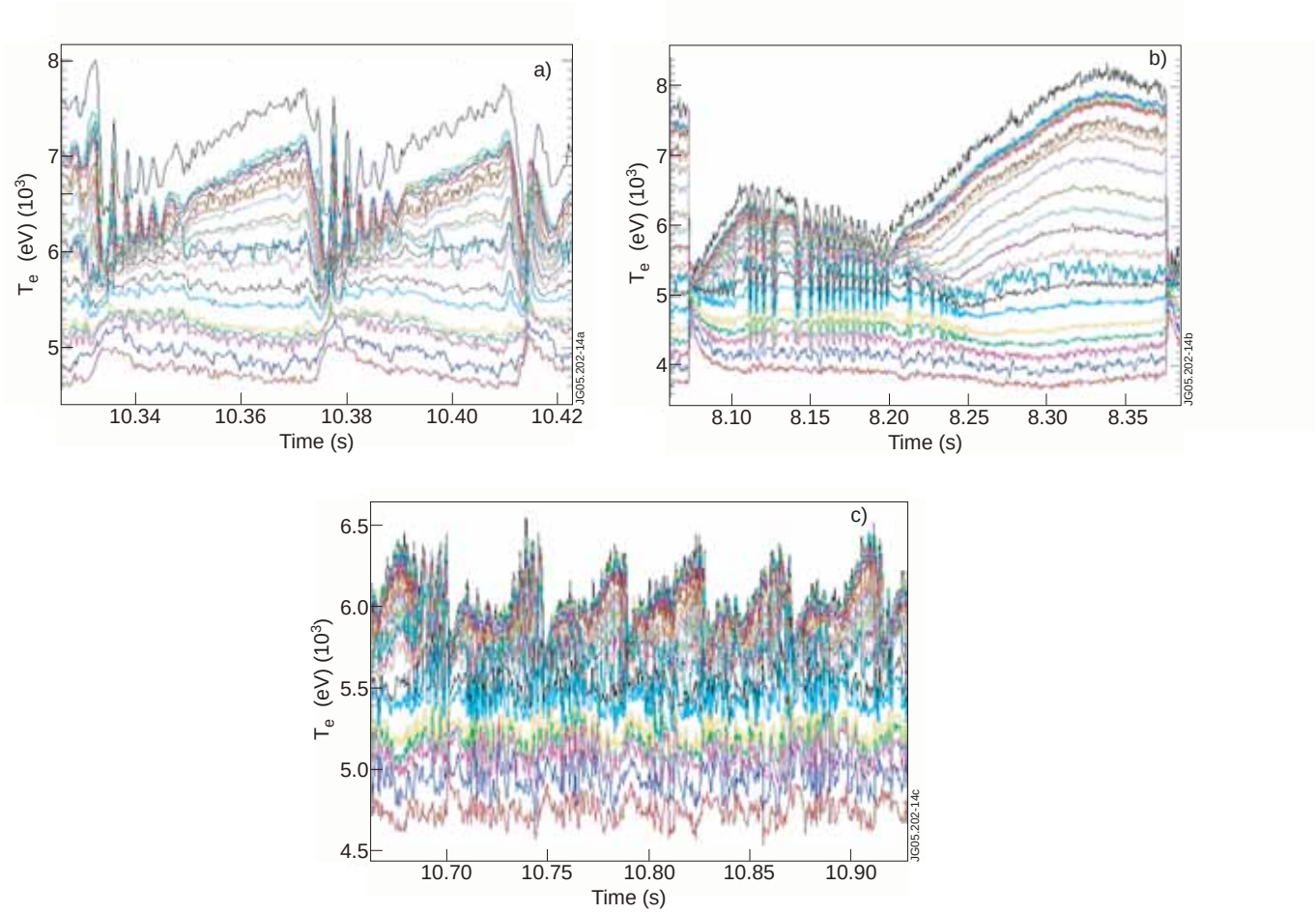

Figure 14(a): T_e measured with ECE in JET Pulse No:62465. Figure 14(b): T_e measured with ECE in Pulse No: 62478 ($+90^0$ ICRH phasing). Figure 14(c): T_e measured with ECE in Pulse No: 62479 (-90^0 ICRH phasing).

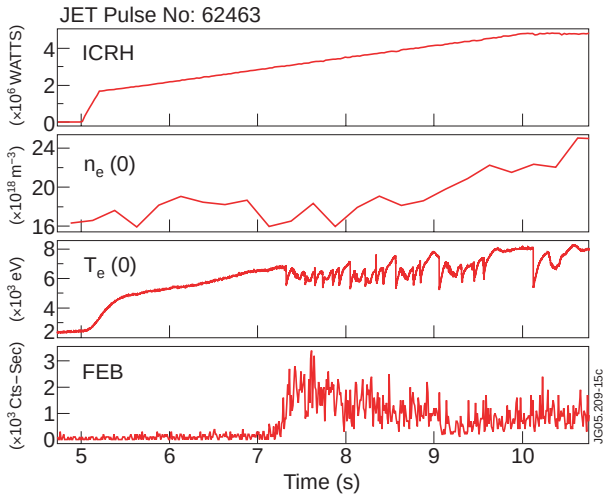

Figure 15: Waveform of ICRH power, central electron density, central electron temperature, and intensity of fast electron Bremsstrahlung emission integrated in the energy range 150-225 keV for central channel 3 of the horizontal FEB camera.

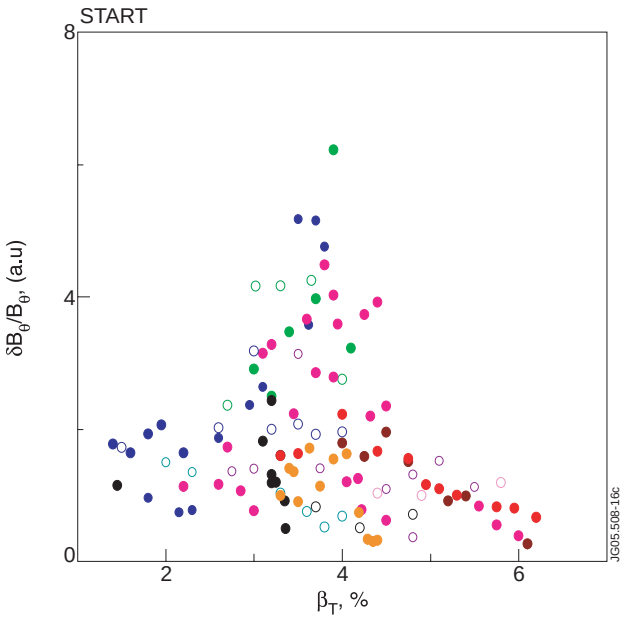

Figure 16: On START, the chirping mode amplitude decreases as beta increases. Different colours indicate different discharges and data for several modes per discharge are plotted.

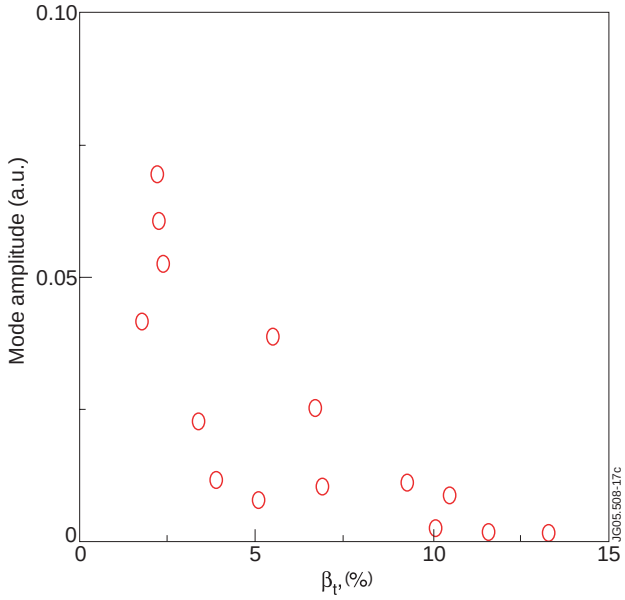

Figure 17: Dependence on β of the maximum amplitude in a single burst of chirping modes, in NBI discharges on MAST.